Uncoupling Endothelial Nitric Oxide Synthase Is Ameliorated by Green Tea in Experimental Diabetes by Re-establishing Tetrahydrobiopterin Levels

Aline M. Faria, Alexandros Papadimitriou, Kamila C. Silva, Jacqueline M. Lopes de Faria, and José B. Lopes de Faria

The current study investigated the potential of green tea (GT) to improve uncoupling of endothelial nitric oxide synthase (eNOS) in diabetic conditions. In rats with streptozotocin-induced diabetes, nitric oxide (NO) bioavailability was reduced by uncoupling eNOS, characterized by a reduction in tetrahydrobiopterin (BH_4) levels and a decrease in the eNOS dimer-to-monomer ratio. GT treatment ameliorated these abnormalities. Moreover, immortalized human mesangial cells (ihMCs) exposed to high glucose (HG) levels exhibited a rise in reactive oxygen species (ROS) and a decline in NO levels, which were reversed with GT. BH_4 and the activity of guanosine triphosphate cyclohydrolase I decreased in ihMCs exposed to HG and was normalized by GT. Exogenous administration of BH_4 in ihMCs reversed the HG-induced rise in ROS and the decline in NO production. However, coadministration of GT with BH_4 did not result in a further reduction in ROS production, suggesting that reduced ROS with GT was indeed secondary to uncoupled eNOS. In summary, GT reversed the diabetes-induced reduction of BH_4 levels, ameliorating uncoupling eNOS, and thus increasing NO bioavailability and reducing oxidative stress, two abnormalities that are involved in the pathogenesis of diabetic nephropathy. ***Diabetes*** **61:1838–1847, 2012**

Oxidative stress has been seen as a critical underlying mechanism causing the microvascular complications of diabetes, including diabetic nephropathy (DN) (1–3). Hyperglycemia is known to increase oxidative stress via the activation of multiple pathways, leading to the generation of superoxide anions and other reactive oxygen species (ROS) in different renal cell types, which thus contributes to renal damage (1,2). Some of these pathways include enhanced activity of the mitochondrial electron transport chain (3), activation of NADPH-oxidase enzyme-induced superoxide formation (2–6), and uncoupling of endothelial nitric oxidase synthase (eNOS) (6). Uncoupled eNOS is a phenomenon characterized by the diversion of electron transfer within the eNOS molecule from L-arginine oxidation, resulting in a reduction of molecular oxygen to form superoxide instead of NO (7). Therefore, uncoupled eNOS contributes not only to increases in ROS formation but also to decreases in NO bioavailability, two conditions involved in the pathogenesis of DN (8). Indeed, eNOS uncoupling has been seen as a major source of local superoxide production in diabetic kidneys (6).

Three main pathways have been identified as the mechanism for uncoupling eNOS: oxidation of tetrahydrobiopterin (BH_4), depletion of L-arginine, and accumulation of methylarginines (9). A recent study has suggested that the balance between NO and superoxide production by eNOS is determined by the levels of BH_4 at its production and stability level (10). BH_4 is synthesized via two main pathways—the de novo synthesis and salvage pathways. The first step involved in the de novo synthesis of BH_4 formation includes a rate-limiting enzyme, such as guanosine triphosphate (GTP) cyclohydrolase I (GTPCH I), which catalyzes the formation of BH_4 from GTP via a series of enzymatic reactions (11). An alternative pathway for BH_4 synthesis has been documented, whereby 7,8-dihydrobiopterin (BH_2) is reduced to BH_4 via dihydrofolate reductase (DHFR), the so-called salvage pathway (12).

A recent study indicated that increased BH_4 oxidation, rather than BH_4 depletion, is the molecular trigger for NO insufficiency in high glucose (HG) conditions (13). Researchers have proposed that the mechanism of decreased BH_4 in diabetes is proteasome-dependent degradation of GTPCH I in BH_4 synthesis (14). To this end, there is evidence that the administration of BH_4 may prevent endothelial dysfunction (15). Therefore, maneuvers that re-establish BH_4 bioavailability with consequent eNOS coupling may be useful in treating DN, a disease characterized by endothelial dysfunction (16).

Tea is considered the second most frequently consumed beverage worldwide, after water (17). Green tea (GT; *Camellia sinensis*) is a rich source of polyphenols, particularly flavonoids, which have been shown to positively affect the modulation of endothelial NO (17). In a double-blind, placebo-controlled study, one of the main components of GT, (-)-epigallo-catechin gallate (EGCG), acutely improved flow-mediated dilation, an estimation of endothelial function in humans (18). In a recent study, GT ameliorated oxidative stress in diabetic rat kidneys via reduced expression of NADPH oxidase 4 (NOX4), and hence superoxide formation (5). The reduction in oxidative stress as a result of GT also contributed to the amelioration of indices of renal injury, such as albuminuria and renal accumulation of collagen IV (5). However, the role of GT in BH_4 synthesis, coupling eNOS, and hence, NO bioavailability under diabetic conditions, has not been evaluated. Therefore, the aim of the present work was to assess the potential of GT to ameliorate BH_4 levels, uncouple eNOS, and NO bioavailability in diabetic conditions using an in vivo model of diabetic spontaneously hypertensive (SHR) rats and an in vitro system of human kidney mesangial cells.

From the Renal Pathophysiology Laboratory, Investigation on Diabetes Complications, Faculty of Medical Sciences, State University of Campinas (Unicamp), Campinas, São Paulo, Brazil.
Corresponding author: José B. Lopes de Faria, jblfaria@fcm.unicamp.br.
Received 22 September 2011 and accepted 29 February 2012.
DOI: 10.2337/db11-1241
This article contains Supplementary Data online at http://diabetes.diabetesjournals.org/lookup/suppl/doi:10.2337/db11-1241/-/DC1.

RESEARCH DESIGN AND METHODS

Reagents. All reagents were purchased from Sigma (St. Louis, MO), unless otherwise stated.

Animals and study design. This study protocol was approved by the local committee for ethics in animal research (CEEA/IB/Unicamp). The SHR rats used in the study were provided by Taconic (Germantown, NY). Experimental diabetes was induced in 12-week-old SHR rats via an intravenous injection of streptozotocin (50 mg/kg in sodium citrate buffer, pH 4.5). The day after diabetes induction, the diabetic rats were randomly assigned to receive or not receive GT (~5 g/kg body weight/day) instead of drinking water. Japanese GT (Midori Industria de Chá) was prepared daily, as we have described before (5). During the study, the diabetic rats received 2 units of insulin (human insulin HI-0310; Lilly), three times per week, subcutaneously. The control rats only received the vehicle. We chose to induce diabetes in SHR rats because they present a more progressive form of renal disease (19), we have a vast experience with this model (2,5,20), and also because of the frequent association of diabetes with hypertension in human diabetic renal disease. After 12 weeks of diabetes induction, the rats were killed, the kidneys were decapsulated and removed, and a piece of the cortex was used for protein isolation. The remaining kidney cortex was snap-frozen at −80°C for future assays.

Renal histopathology. The kidney was embedded in paraffin, and 3-μm sections were cut and stained with periodic acid–Schiff. Matrix mesangial expansion, quantified by Leica Application Suite (LAS Image Analysis), was derived from assessment of 30 glomeruli from each rat.

Human mesangial cell culture. Immortalized human mesangial cells (ihMCs; passage 10 to 20) from Dr. Bernhard Banas (Nephrology Center, Medical Policlinic, Ludwig-Maximilian University of Munich, Germany) were provided by Dr. Nestor Schor (Department of Medicine, Nephrology Division, Federal University of São Paulo, Brazil). The ihMCs were cultured as described previously (21). The cells were kept without serum in normal glucose (NG, 5.5 mmol/L) and HG (30 mmol/L) mediums in the presence of various treatments for an additional 24 h. The concentrations of treatments used in the HG medium in all experiments were chosen after completing a thiazolyl blue tetrazolium bromide assay (data not shown).

Western blotting analysis. The kidney cortex or ihMCs were lysed in a radioimmunoprecipitation assay buffer supplemented with a protease inhibitor cocktail (Complete; Boehringer-Mannheim, Indianapolis, IN). The samples and Western blots were prepared as previously described (5). The Bradford method (22) was used for protein quantification. The following primary antibodies were used: rabbit polyclonal anti-eNOS (Santa Cruz) rabbit polyclonal p-eNOS Thr495, and rabbit polyclonal p-eNOS Ser1177 (Cell Signaling Technology). Equal loading and transfer was achieved by reprobing the membranes for β-actin. To determine eNOS dimer-to-monomer ratio, sample preparation and Western blot was performed as previously described (23).

TABLE 1
Physiologic characteristics of studied animals

SHR groups	Body weight (g) Initial	Body weight (g) Final	SBP mmHg	Glycemia mmol/L
CT	277.2 ± 17	345.5 ± 13	204.3 ± 10	8.4 ± 1
DM	277.6 ± 7	192.2 ± 38*	203.5 ± 8	29.5 ± 2*
DM+GT	269.7 ± 15	194.9 ± 25*	198.9 ± 10	30.5 ± 5*

CT, control; DM, diabetic; DM+GT, diabetic treated with GT; SBP, systolic blood pressure. *P < 0.0001 vs. CT group.

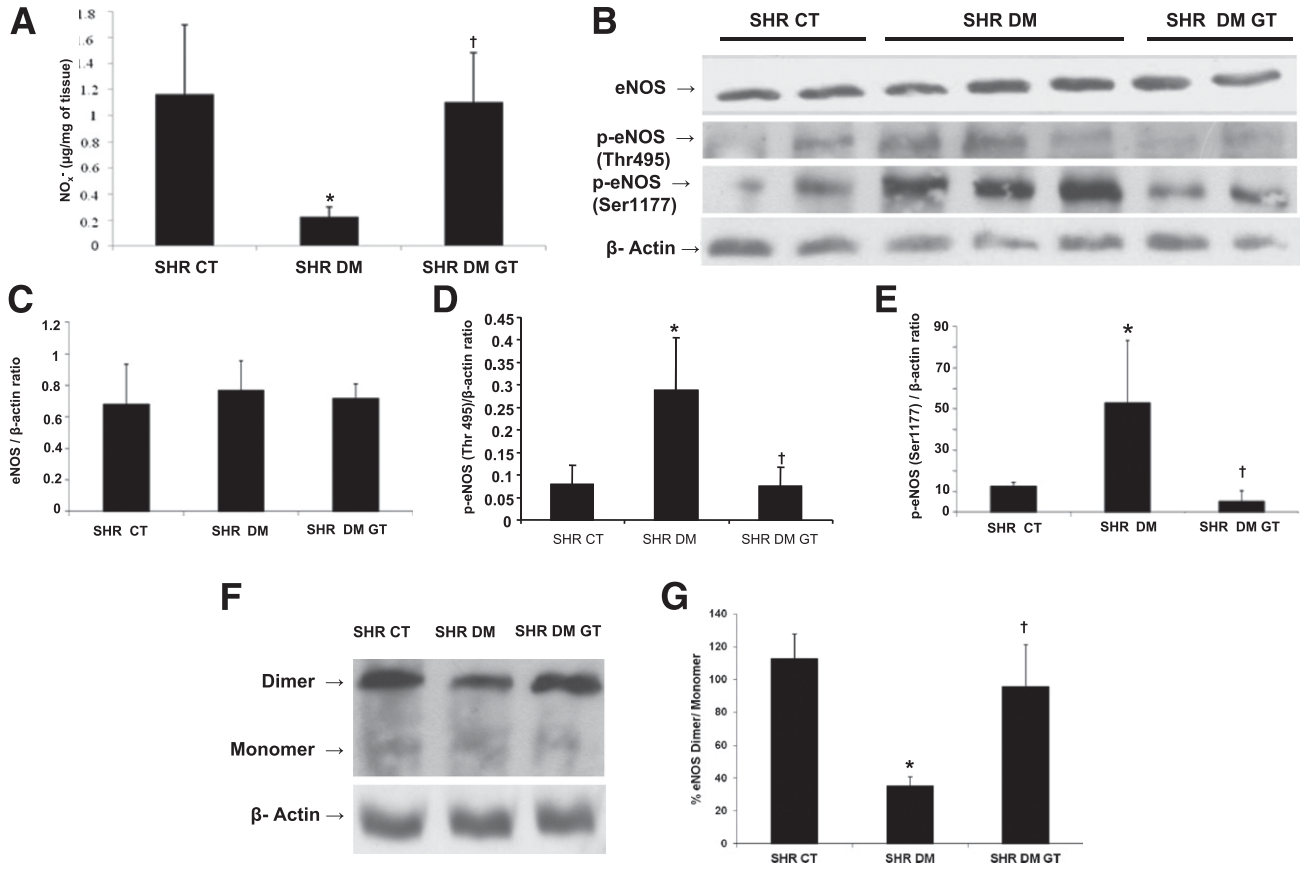

FIG. 1. *A*: Nitrite (NO_2^-) and nitrate (NO_3^-), the stable NO end products, were quantified as a measurement of NO levels in renal cortical homogenates by Griess reaction in SHR rats: control (CT), diabetic (DM), and DM treated with GT (DM GT). Results were corrected for the protein concentration and are expressed as NOx^- (μmol/mg of protein). *P = 0.02 vs. SHR CT; †P = 0.05 vs. SHR DM. *B*: Representative Western blots of the renal cortical eNOS and p-eNOS (Thr495) expression from SHR CT rats, SHR DM rats, and SHR DM GT. Densitometric analysis of the eNOS–to–β-actin ratio (*C*), phosphorylated (p)-eNOS (Thr495)-to-β-actin ratio (*P = 0.002 vs. SHR CT, †P = 0.005 vs. SHR DM) (*D*), and p-eNOS (Ser1177)–to–β-actin ratio (*P = 0.03 vs. SHR CT, †P = 0.05 vs. SHR DM) (*E*), in the three SHR rat groups. Bars represent means ± SD. *F*: Representative Western blots of the renal cortical of eNOS dimer and monomer expression from SHR CT rats, SHR DM rats, and SHR DM GT rats. *G*: Densitometric analysis of the percentage of eNOS dimer-to-monomer ratio. *P = 0.02 vs. SHR CT. †P = 0.05 vs. SHR DM.

NO_X^- analysis by Griess reaction. The analysis of NO end products, such as nitrate and nitrite (NO_X^-), was evaluated by the Griess reaction, as previously described (24). Briefly, the renal cortex was lysed in 300 μL extraction buffer (50 mmol/L Tris-HCl [pH 7.4], 1 mmol/L EDTA, 10 mmol/L dithiothreitol). The kidney cortex lysate was then deproteinized by 0.6 mol/L trichloroacetic acid for 1 h at 4°C, and the samples were incubated with chloride vanadium in 1:1 proportion for 15 min. Then, 0.1% *N*-naftil-etilenodiamine and 2% sulfanilamide were added to the samples for 30 min in the dark, at room temperature. The samples were read by a spectrophotometer (Powerwave XS2, Biotek) at 540-nm absorbance.

Measurement of intracellular levels of biopterins. Oxidized and reduced forms of biopterins were analyzed by the differential oxidation method and were determined according to a previously described method (25), with some modifications (26). The renal cortex and ihMCs were lysed in a 500 μL extraction buffer (50 mmol/L Tris-HCl [pH 7.4], 1 mmol/L EDTA, 10 mmol/L dithiothreitol). The samples were injected into an ultraperformance liquid chromatography system (Waters). BH_4 concentration, expressed as picomoles or nanomoles per milligram of protein, was calculated by subtracting BH_2 plus biopterin from total biopterins. The percentage of BH_4 oxidation was calculated using the following formula: Percentage of BH_4 oxidation = 100 − (BH_4 levels × 100/biopterin levels)

Measurement of GTPCH activity. GTPCH activity was measured using the high performance liquid chromatography (HPLC) method, as described previously (27).

2′,7′-Dichlorodihydrofluorescein diacetate (H_2DCF-DA) measurement of ROS production. Intracellular ROS levels were measured by H_2DCF-DA. Qualitative assessment of ROS was carried out in the ihMCs after they were kept for 24 h with the NG and HG mediums alone or in the presence of GT (100 μg/mL) and different treatments. To quantify the ROS levels, the same procedure used for the qualitative analysis of ROS was applied. Relative fluorescence was measured using a fluorescence plate reader (SynergyMx; Biotek) at excitation and emission wavelengths of 485 and 528 nm, respectively. The relative fluorescence values were corrected by the number of cells in each treatment.

Diaminorhodamine-4M AM and 4,5 diamino-fluorescein diacetate (DAF)-2DA measurement of NO. Intracellular NO was measured in ihMCs via diaminorhodamine-4M AM (Alexis Biochemicals, Switzerland). To quantify NO levels, the same procedure used for the qualitative analysis of NO was applied, but using the probe DAF-2DA. Relative fluorescence was measured using a fluorescence plate reader (SynergyMx; Biotek) at excitation and emission wavelengths of 495 and 515 nm, respectively. The relative fluorescence values were corrected by the number of cells in each treatment.

Estimation of EGCG in GT. The estimation of EGCG in GT was assessed by HPLC (Waters) using an EGCG standard, as previously reported (28).

Statistical analysis. All experiments were independently performed three times and the results are expressed as means ± SD. One-way ANOVA, followed by the Bonferroni test, were used to compare the groups. A value of $P < 0.05$ was considered significant. All analyses were performed using StatView software (SAS Institute, Inc., Cary, NC).

RESULTS

Physiologic characteristics. Body weight gain was lower in the diabetic rats than in the control rats. Systolic blood pressure was similar in all groups. Blood glucose concentration was greater in the diabetic rats than in the control rats but was not affected by GT (Table 1).

Renal histopathology. Matrix mesangial expansion was greater in diabetic SHR rats than in control rats. This abnormality was reversed by GT treatment (P = 0.03; Supplementary Fig. 1*A* and *B*).

NO_X^- levels and eNOS expression in renal cortical tissue. Kidney homogenates from the diabetic rats had significantly lower levels of NO_X^- compared with the control rats (P = 0.02), which was reversed by GT treatment (P = 0.05; Fig. 1*A*).

Modulation of NO bioavailability was also assessed via analysis of eNOS expression and its phosphorylation status. Renal cortical expression of eNOS did not differ between the studied rats (Fig. 1*B* and *C*). Diabetic SHR rats demonstrated increased phospho-Thr495 eNOS expression (P = 0.002), which was reversed by GT treatment (P = 0.005;

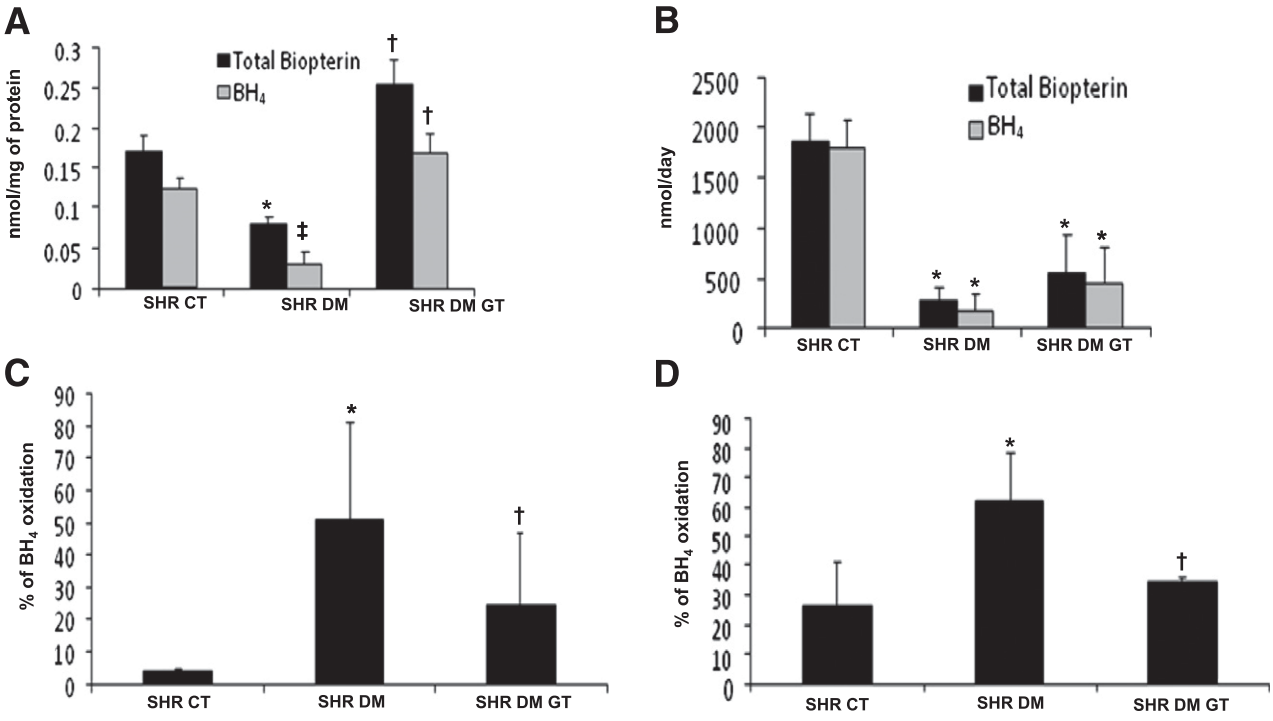

FIG. 2. Ultraperformance liquid chromatography was used to analyze total biopterin and BH_4 expression in SHR control (CT) rats, diabetic (DM) rats, and DM rats fed GT (DM GT) in the renal cortex (*A*) and urine (*B*). Results in the renal cortex were corrected for the protein concentration and are expressed as nmol/mg protein. *P = 0.002 vs. SHR CT. †P < 0.0001 vs. SHR DM. ‡P < 0.0001 vs. SHR CT. Results in the urine were corrected for 24-h urine volume. *P < 0.0001 vs. SHR CT. Representative graphs show the of percentage of BH_4 to BH_2 oxidation in the renal cortex (*C*) (*P = 0.01 vs. SHR CT, †P = 0.03 vs. SHR DM) and in the urine (*D*) (*P = 0.004 vs. SHR CT, †P = 0.05 vs. SHR DM).

Fig. 1*B* and *D*). Thr495 represents the major negative regulatory site of eNOS and is constitutively phosphorylated in cultures in many endothelial cell types (29). However, the expression of phospho-Ser1177 eNOS in renal cortical homogenates increased in the diabetic SHR rats ($P = 0.03$), and GT consumption reduced its expression ($P = 0.05$; Fig. 1*B* and *E*). Ser1177 thus appears to be the most important positive regulatory domain in eNOS. Finally, the percentage of the dimer-to-monomer ratio, an indicator of eNOS uncoupling, showed a significant decrease in diabetic rats ($P = 0.02$), which was re-established by GT treatment ($P = 0.05$; Fig. 1*F* and *G*).

Urinary and renal cortical levels of total biopterin and BH_4 and the percentage of BH_4 oxidation in the control and diabetic animals. BH_4 and total biopterin levels in renal cortical homogenates ($P < 0.002$) and urine ($P < 0.0001$) decreased in the diabetic SHR rats compared with the control SHR rats (Fig. 2*A* and *B*). GT significantly abrogated the reduction of BH_4 in the renal cortex ($P = 0.0008$), and the urinary levels of BH_4 with GT tended to increase in the diabetic SHR rats (Fig. 2*A* and *B*). Similar results were obtained for total biopterin levels (Fig. 2*A* and *B*). Moreover, the percentage of oxidation of BH_4 to BH_2 was increased in the diabetic rats compared with the control rats in the renal cortex ($P = 0.03$) and urine ($P = 0.05$), whereas GT treatment abolished the oxidation of BH_4 (Fig. 2*C* and *D*).

Effects of HG and GT on NO production in ihMCs. Qualitative and quantitative analyses of NO production showed that the ihMCs kept in the HG medium for 24 h had a significant reduction ($P = 0.03$) in fluorescence intensity compared with cells kept in the NG medium, whereas GT (100 μg/mL) reversed the HG-induced reduction in NO ($P = 0.02$; Fig. 3*A* and *B*). Western blot analysis revealed that the eNOS expression was similar in ihMCs cultured in NG, HG, or HG with GT (Fig. 3*C* and *D*). However, the eNOS dimer-to-monomer ratio was decreased in ihMCs cultured under HG ($P = 0.04$), and this alteration was reversed by GT treatment ($P = 0.05$; Fig. 3*E* and *F*).

Effects of HG in ROS production in ihMCs. Qualitative and quantitative analyses (Fig. 4*A* and *B*) showed a significant rise in ROS production after the ihMCs were exposed to HG levels for 24 h ($P = 0.0001$) compared with NG levels. To evaluate the sources involved in the HG-induced ROS production in the ihMCs, we analyzed ROS production at HG in the presence of diphenyleneiodonium (DPI; 50 nmol/L, a blocker of NADPH-oxidase), L-N^G-nitro-L-arginine methyl ester (L-NAME; 100 μmol/L, an inhibitor

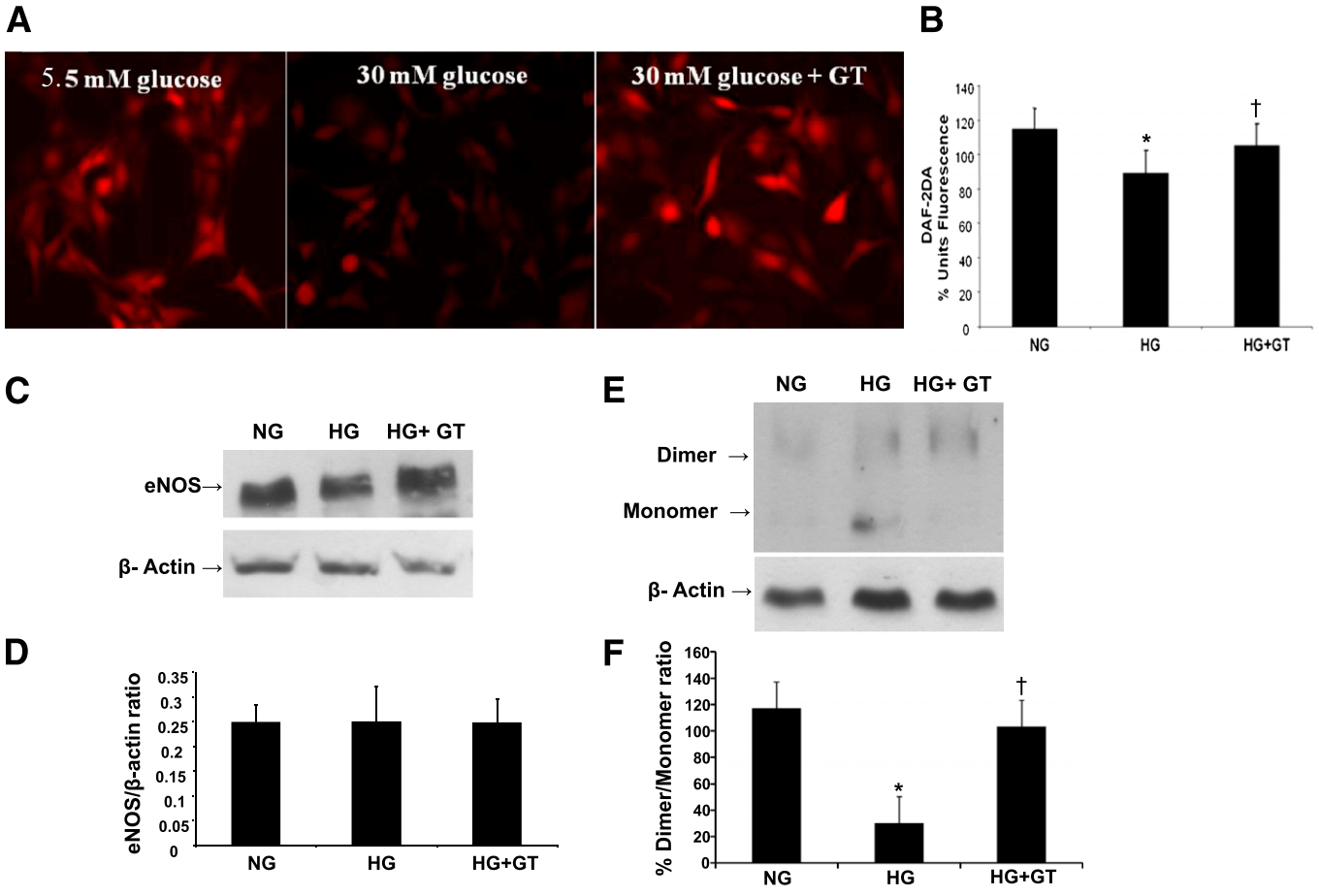

FIG. 3. ***A*: Representative photomicrographs of diaminorhodamine-4M AM indicating NO production. ihMCs were cultured for 24 h in NG (5.5 mmol/L), HG (30 mmol/L), and HG with GT (100 μg/mL). *B*: Quantification of NO levels in ihMCs via DAF-2DA. Values are mean ± SD and expressed as the percentage of fluorescence. Values were corrected by the number of cells at the end of each treatment. *$P = 0.03$ vs. NG. †$P = 0.02$ vs. HG. *C*: Representative Western blots of the ihMCs of eNOS expression from ihMCs cultured under NG, HG, and HG treated with GT for 24 h. *D*: Densitometric analysis of the eNOS–to–β-actin ratio. *E*: Representative Western blots of the ihMCs of eNOS dimer and monomer expression from ihMCs cultured under NG, HG, and HG treated with GT for 24 h. *F*: Densitometric analysis of the percentage of eNOS dimer-to-monomer ratio. *$P = 0.04$ vs. NG. †$P = 0.05$ vs. HG. (A high-quality digital representation of this figure is available in the online issue.)**

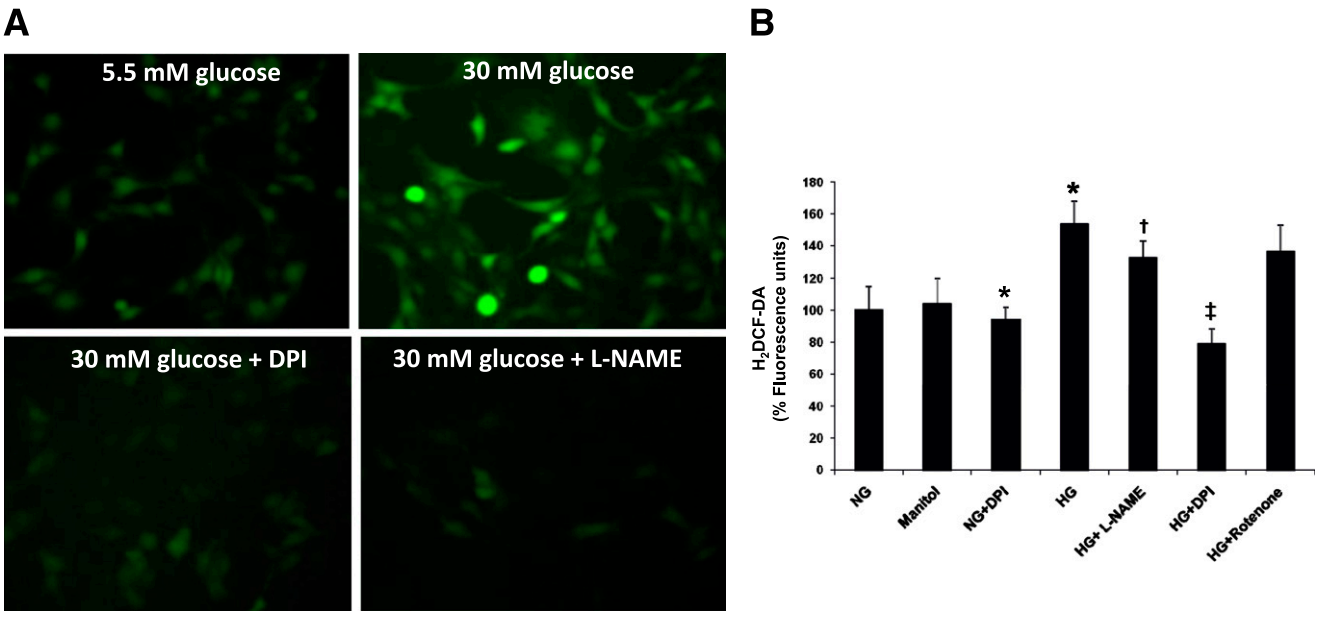

FIG. 4. *A*: Representative photomicrographs of ihMCs probe with H_2DCF-DA indicating ROS production. Cells were cultured in NG, HG, HG plus GT, HG plus DPI, and HG plus L-NAME. *B*: Quantification of total intracellular ROS levels and an assessment of enzymatic sources of ROS production in ihMCs. HMCs were cultured for 24 h in NG (5.5 mmol/L) and HG (30 mmol/L) in the presence and absence of GT. Mannitol was used as an osmotic control; L-NAME (an inhibitor of NOS), DPI (an inhibitor of NADPH oxidase), and rotenone (an inhibitor of mitochondrial complex I) were also used at HG levels to define the enzymatic sources of ROS production. Values are mean ± SD and expressed as the percentage of fluorescence. Values were corrected for the number of cells at the end of each treatment. *$P < 0.0001$ vs. NG. †$P = 0.04$ vs. HG. ‡$P = 0.03$ vs. HG. (A high-quality digital representation of this figure is available in the online issue.)

of NOS enzymes), and rotenone (10 μmol/L, an inhibitor of mitochondria electron transport complex I). Fluorescent microscope (Fig. 4*A*) and fluorometer (Fig. 4*B*) data showed that DPI reversed HG-induced ROS production to levels lower than those of NG ($P = 0.03$), suggesting that NADPH oxidase is one main source of superoxide in ihMCs. DPI reduces ROS production even in cells cultured in NG. This observation may explain the reduction of ROS in cells under HG to below control levels (Fig. 4*B*). Furthermore, incubation of ihMC with L-NAME significantly reduced HG-induced superoxide production ($P = 0.04$), suggesting that eNOS uncoupling is an important source of ROS production. Finally, incubation with rotenone reduced HG-induced superoxide production, although it failed to reach statistical significance ($P = 0.07$). Mannitol (30 mmol/L), which was used as an osmotic control, did not alter ROS production. These results imply that NADPH oxidase and uncoupling eNOS are both important sources in the HG-induced ROS production in ihMCs.

Effects of BH_4 in ROS and NO production at HG in ihMCs. We observed a significant reduction in total biopterin and BH_4 levels in ihMCs kept in the HG medium ($P = 0.05$) compared with cells in the NG medium (Fig. 5*A*), which was reversed by GT ($P = 0.04$). Furthermore, there was an increase in oxidation of BH_4 to BH_2 in cells kept in the HG medium ($P = 0.01$), and this also was reversed after GT treatment ($P = 0.01$; Fig. 5*B*). We next assessed the role of BH_4 in ROS and NO production in ihMCs. Exogenous administration of BH_4 in ihMCs kept in the HG medium (Fig. 5*C*) reduced the HG-induced rise in ROS production in a concentration-dependent manner, although this only reached significance at 100 μmol/L ($P = 0.004$). Moreover, measurement of NO via DAF-2DA (Fig. 5*D*) showed that BH_4 at all concentrations used ($P = 0.001$) reversed the HG-induced decline in NO production ($P = 0.007$). These findings may imply that a reduction in BH_4 levels may be involved in HG-induced ROS production and a decline in NO formation.

Effects of HG and GT in GTPCH I activity and DHFR function in ihMCs. To investigate the mode of action of HG-induced reduction in BH_4 levels, we next used HPLC to assess the activity of GTPCH I. Our results showed that there was a significant reduction in GTPCH I activity ($P = 0.03$) in ihMCs kept in the HG medium (Fig. 6*A*) compared with cells kept in the NG medium. Interestingly, GT reversed the HG-induced decline in GTPCH I activity ($P = 0.009$; Fig. 6*A*). To further assess the hypothesis that GT re-established GTPCH I activity in ihMCs, we cultured these cells in HG with GT (100 μg/mL), and after 1 h, we supplemented the medium with 2,4-diamino-6-hydroxypyrimidine, an inhibitor of GTPCH I. We observed that the presence of the GTPCH I inhibitor abrogated the beneficial effect of GT (i.e., it increases ROS production [Fig. 6*E*] and decreases NO bioavailability [Fig. 6*F*]), in a concentration-dependent manner. These observations further support the concept that GT improved NOS uncoupling by re-establishing the GTPCH I activity and synthesis of BH_4.

To test the integrity of BH_2-to-BH_4 recycling in ihMC under HG, the cells were kept with HG in the presence of BH_2, and ROS production was evaluated. Analysis (Fig. 6*B* and *C*) of ROS production showed that BH_2 reduced the HG-induced ROS production in a concentration-dependent manner, although this was only significant at 10 μmol/L and 100 μmol/L ($P = 0.0001$). Analysis of NO production showed that the exogenous administration of BH_2 significantly blunted the HG-induced decline of NO production ($P = 0.03$; Fig. 6*D*). These data may further suggest that HG in ihMCs reduces the production of BH_4 via a decline in GTPCH I activity at the de novo synthesis pathway of BH_4 formation. However, HG does not affect BH_4 production via

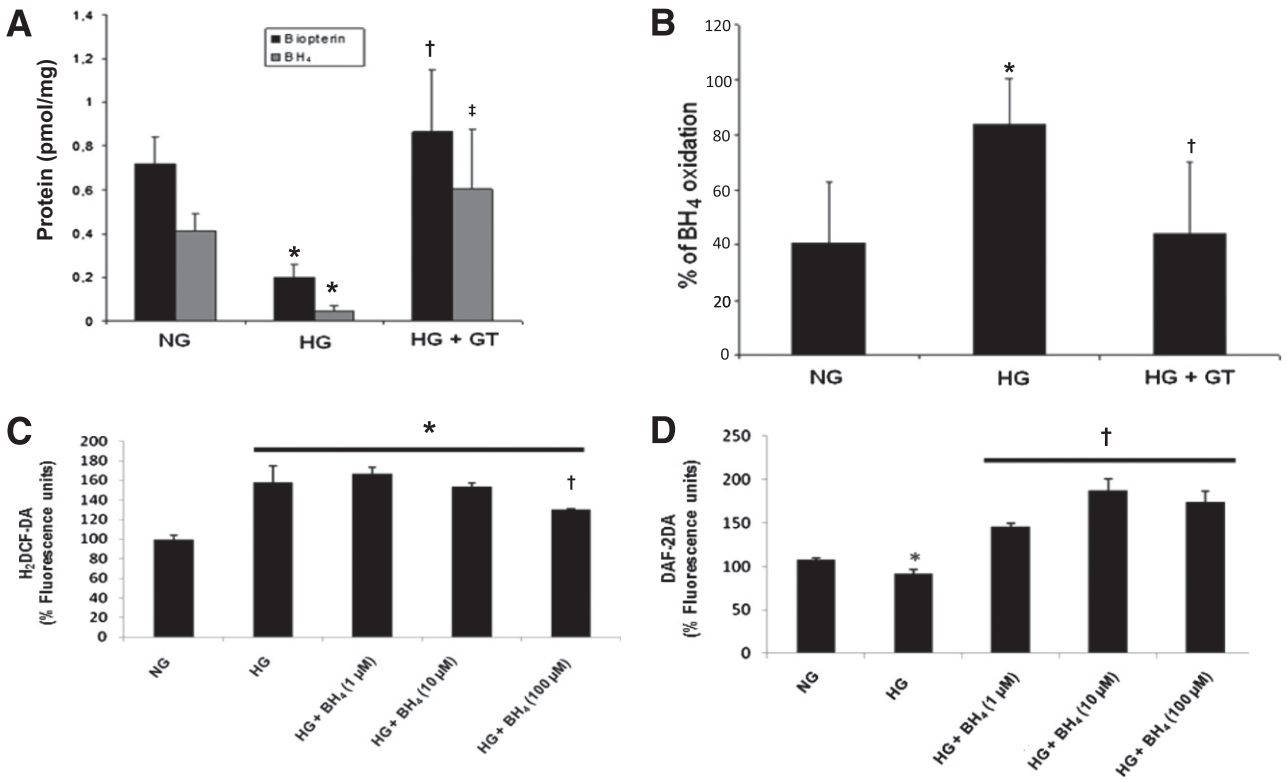

FIG. 5. ***A*****: Total biopterin and BH_4 expression analysis by ultraperformance liquid chromatography in ihMC lysate. Results were corrected for the protein concentration and expressed as nmol/mg protein. *P = 0.05 vs. NG. †P = 0.02 vs. HG. ‡P = 0.04 vs. HG.** ***B*****: Representative graphs of percentage of BH_4 to BH_2 oxidation in ihMC lysate. *P = 0.01 vs. NG. †P = 0.01 vs. HG.** ***C*****: Quantification of total intracellular ROS levels by H_2DCF-DA via a fluorimeter after incubation of ihMCs for 24 h in NG and HG mediums in the presence also of BH_4 (1, 10, and 100 μmol/L). *P = 0.0001 vs. NG. †P = 0.004 vs. HG.** ***D*****: NO levels were also quantified after incubation with DAF-2DA via a fluorimeter. *P = 0.007 vs. NG. †P = 0.001 vs. HG. The bars represent mean ± SD. Values are expressed as the percentage of fluorescence units and were corrected by the number of cells at the end of each treatment.**

the recycling pathway because BH_2 ameliorated both the HG-induced rise in ROS production and the decline in NO formation.

Effects of GT in ROS production at HG in ihMCs. In ihMCs, assessment of ROS production showed that GT reversed the HG-induced rise in ROS formation to NG levels (Fig. 7*A* and *B*; P = 0.0001). Cotreatment of ihMCs with GT and BH_4 (Fig. 7*C*) did not confer an additional reduction in ROS production compared with GT treatment alone. This suggests that GT may inhibit HG-induced ROS production through a rise in BH_4 levels.

Content of EGCG in GT and the EGCG effect in ihMCs. When compared with the EGCG standard, we identified this polyphenol as an important constituent of GT. The EGCG retention time was 8.891 min (Supplementary Fig. 2*A*), consistent with the main peak retention time of 8.894 min observed in GT (Supplementary Fig. 2*B*). Assessment of the effect of EGCG in ihMCs exposed to HG has shown that this component of GT can reduce ROS production (Supplementary Fig. 2*C*) and increase NO bioavailability (Supplementary Fig. 2*D*). These observations suggest that the main effect of GT may be attributed, at least partly, to EGCG.

DISCUSSION

The current study aimed to explore the potential of GT to ameliorate kidney-uncoupling eNOS in diabetic conditions. We also investigated the mechanisms by which GT reversed uncoupling eNOS. We observed, both in vivo and in vitro, an uncoupling of eNOS secondary to a reduction of BH_4 and elevation of its oxidized form with a consequent decrease in NO and an increase in oxidative stress. GT re-established the levels of BH_4, reduced its oxidized form, coupled eNOS, and consequently, increased NO bioavailability and reduced oxidative stress. Our in vitro data also suggest that the re-establishment of GTPCH I activity is the main mechanism by which GT increased BH_4 and coupled eNOS. These observations are of great interest. First, they reinforce the importance of uncoupling eNOS and BH_4 synthesis/oxidation in reducing NO bioavailability, and increase oxidative stress, two conditions involved in the pathogenesis of DN (1–8). In addition, the mechanism by which GT can couple eNOS in diabetes is described for the first time. Together with previous observations that GT can reduce oxidative stress and improve indices of DN in rats (5), data from this translational study demonstrate the possible beneficial use of GT or its main flavonol, EGCG, in patients with DN.

Bioavailability of NO in the diabetic kidney has been a subject of major controversy (7,8). Earlier studies have suggested that NO production increases and contributes to glomerular hyperfiltration in short-term diabetes (30,31). More recently, it has been suggested that endothelial dysfunction, which is often defined as a decrease in the bioavailability of endothelial-derived NO, is a preponderant factor in diabetes and contributes to the pathogenesis of DN (6–8,17). To this end, researchers have demonstrated that the knockout of eNOS in diabetic mice leads to severe histologic lesions in the kidney that resemble the lesions seen in human DN but which are not seen in control wild-type

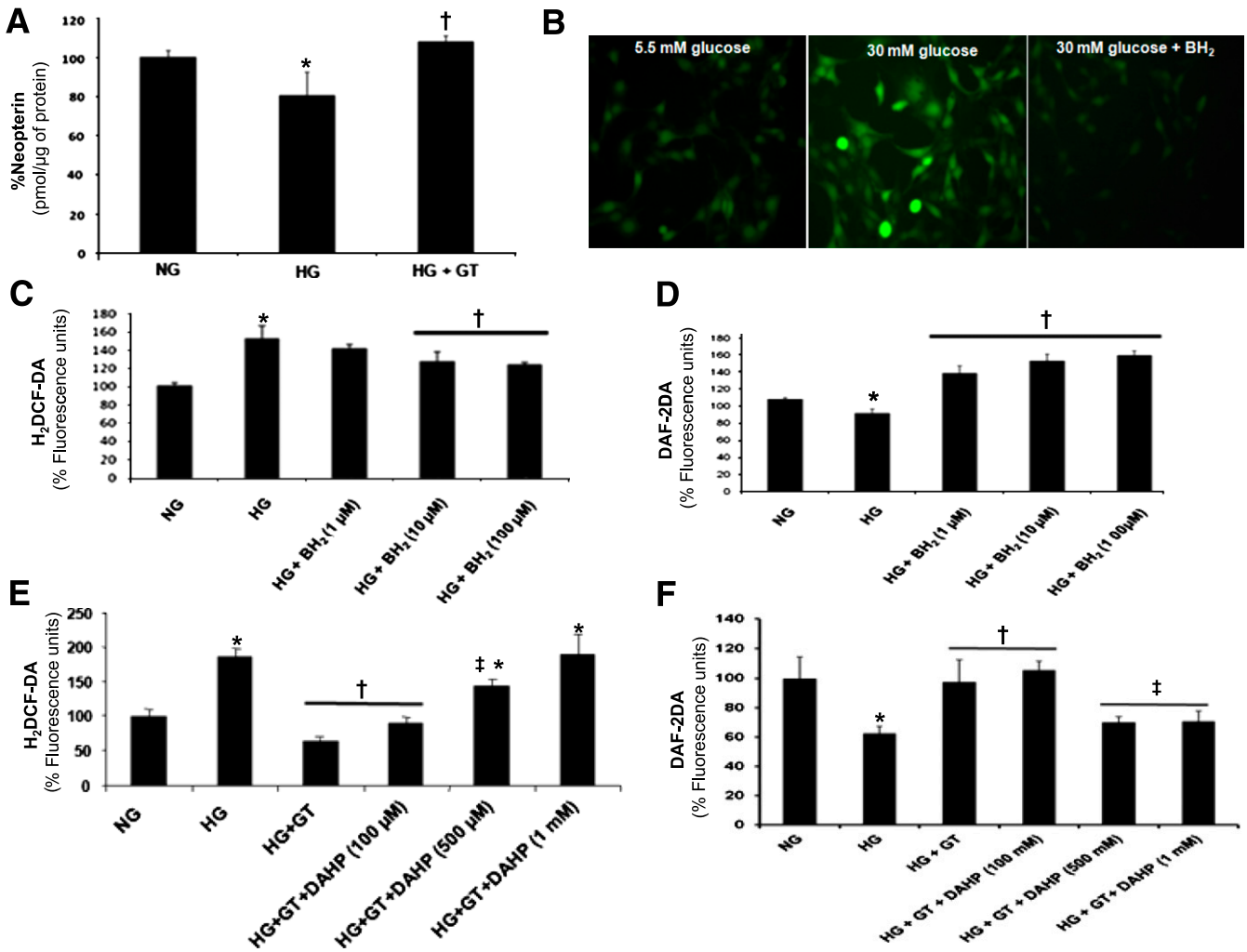

FIG. 6. ***A*****: GTPCH I activity was measured in HPLC by the concentration of neopterin in cell lysate. Results were corrected for the protein concentration and expressed as the percentage of pmol/μg protein. The levels of neopterin indicate GTPCH activity. The ihMCs were cultured for 24 h in NG (5.5 mmol/L), HG (30 mmol/L), and HG with GT (100 μg/mL). *P = 0.03 vs. NG. †P = 0.009 vs. HG. *B*: Representative photomicrographs of H_2DCF-DA in ihMCs indicating ROS production. ihMCs were kept for 24 h in NG and in HG medium in the presence also of BH_2 (10 μmol/L). *C*: ROS measurement in ihMCs supplemented with BH_2 (1, 10, and 100 μmol/L). *P = 0.0001 vs. NG. †P = 0.03 vs. HG. *D*: Quantitative analysis of intracellular NO levels were also carried out after incubation with DAF-2DA. *P = 0.007 vs. NG. †P = 0.001 vs. HG. ROS measurement in ihMCs supplemented with BH_2 (1, 10, and 100 μmol/L). *P = 0.0001 vs. NG. †P = 0.03 vs. HG. *E*: ROS measurement in ihMCs pretreated with HG and GT and supplemented with 2,4-diamino-6-hydroxypyrimidine (DAHP; 100 μmol/L, 500 μmol/L, and 1 mmol/L). *P = 0.0001 vs. NG. †P = 0.0001 vs. HG. ‡P = 0.0003 vs. HG. *F*: Quantitative analysis of intracellular NO levels in ihMCs pretreated with HG and GT and supplemented with DAHP. *P = 0.0004 vs. NG. †P = 0.0001 vs. HG. ‡P = 0.002 vs. NG. The bars represent mean ± SD. Values are expressed as the percentage of fluorescence units and were corrected for the number of cells at the end of each treatment. (A high-quality digital representation of this figure is available in the online issue.)**

diabetic mice (32). In addition, hypertensive type 2 individuals subjected to an acute reduction in NO bioavailability, by means of blockade of NO synthesis with L-NAME, displayed an elevated albumin excretion rate, a hallmark of DN (33). Therefore, it seems that a reduction in NO bioavailability is the predominant abnormality in DM.

It has become apparent that eNOS phosphorylation at Thr495 or Ser1177, rather than eNOS expression, are crucial parameters in estimating NOS production by eNOS (7,8). Interestingly, in our diabetic rats, we observed an increase in inactivation of eNOS via a rise in phosphorylated eNOS at Thr495, which is known to lead to a reduction in electron transfer in eNOS, thus diminishing NO production (34). Surprisingly, we also observed in the same model a rise in the expression of phosphorylated eNOS at Ser1177, which is known to enhance eNOS activity (8). These observations are in agreement with a recent study showing that phosphorylation at Thr495 results in a less active eNOS, even in the context of phosphorylation of eNOS at Ser1177 (35). In our study, GT reversed diabetes-induced alterations in phosphorylated Th495, Ser1177, eNOS, and the dimer-to-monomer ratio, and hence, improved NO bioavailability.

Previous studies have shown that enzymatic coupling of eNOS by BH_4 plays a critical role in the maintenance of NO bioavailability (6,12,16,36,37); for example, endothelial function improved after the exogenous administration of BH_4 in stroke-prone SHR rats via an improvement of eNOS coupling, and hence, a rise in NO bioavailability (37). In our studies, we observed a reduction in BH_4 levels and a rise in the oxidation rate of BH_4 to BH_2 in the renal cortex and urine of diabetic SHR rats. A recent study suggested that BH_4 oxidation, rather than decreased BH_4, is the main determinant of uncoupling eNOS (11,38). In our study, GT

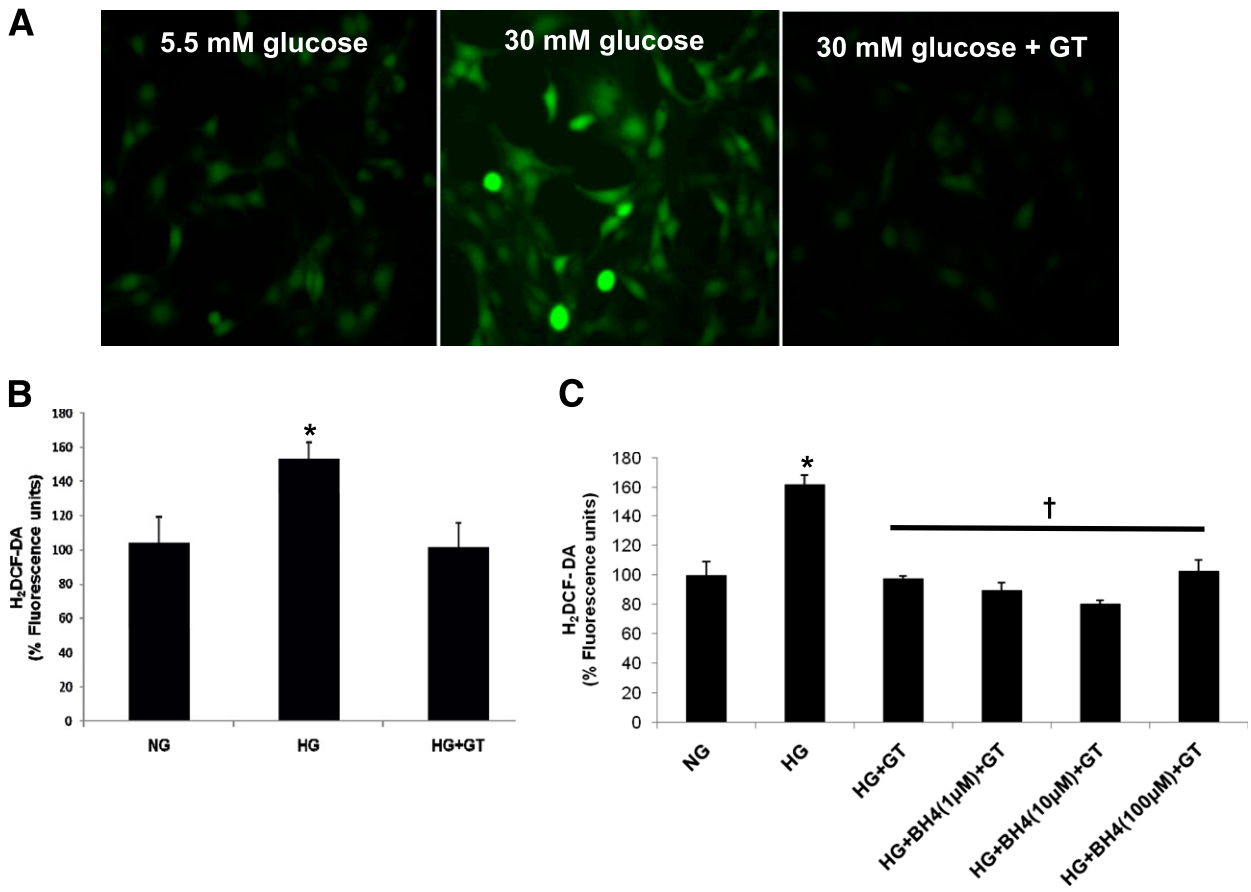

FIG. 7. *A*: **Representative photomicrographs of H_2DCF-DA in ihMCs indicating ROS production. ihMCs were kept for 24 h in NG and HG mediums in the presence also of GT (100 μg/mL).** *B*: **Total intracellular ROS levels by H_2DCF-DA was quantified via a fluorimeter. *P = 0.0001 vs. NG. †P = 0.0001 vs. HG.** *C*: **ihMCs were cultured in HG and supplemented with GT (100 μg/mL) and BH_4, followed by measurement of intracellular ROS by H_2DCF-DA. *P < 0.0001 vs. NG. †P < 0.0001 vs. HG. The bars represent mean ± SD. Values are expressed as the percentage of fluorescence units. (A high-quality digital representation of this figure is available in the online issue.)**

treatment restored the levels of BH_4 and the diabetes-induced oxidation of BH_4 to BH_2 in the renal cortex and urine of diabetic SHR rats. Therefore, GT seems to reverse diabetes-induced eNOS uncoupling, thereby increasing NO bioavailability via a rise in BH_4 availability. This is further supported by our observation that cotreatment of GT and BH_4 did not confer additional protection against HG-induced ROS production compared with GT treatment alone. The ihMCs exposed to HG displayed a rise in ROS production and a decline in intracellular NO production.

Two sources appeared to mediate HG-induced ROS production—NADPH oxidase and uncoupled eNOS—because blocking each one abolished the HG-induced rise in ROS production. Our studies are in agreement with previous work showing that uncoupling eNOS and NADPH oxidase in the glomeruli of rats with experimental DN are the major sources of superoxide mediated by the loss of BH_4 availability (6). In agreement with the importance of reduction in BH_4 availability, exogenous administration of BH_4 in ihMCs abolished ROS production and reversed the decline of NO under HG levels. This finding suggests that ihMCs kept in HG mediums exhibit low levels of BH_4, leading to uncoupling of eNOS, a subsequent rise in ROS, and a decline in NO levels. This is further supported by our finding that BH_4 levels decreased and the oxidation of BH_4 rose to BH_2 in ihMCs kept in the HG medium.

Our present work further showed that ihMCs kept in the HG medium exhibited reduced levels of BH_4 compared with cells kept in the NG medium, due to the diminished de novo synthesis pathway of BH_4 formation, because activity of GTPCH I was reduced in cells cultured in HG. Diminished GTPCH I activity has also been reported in rats with experimental DN, leading to reduced BH_4 formation via the de novo synthesis (39). In addition, the observation that a GTCH I blocker abrogated the effect of GT in ROS and NO production in ihMCs exposed to HG and treated with GT further supports the concept that GT acts by improving GTPCH I activity. Our work also indicated that the recycling pathway of BH_4 is probably preserved in ihMCs exposed to HG because BH_2 supplementation decreased ROS and increased NO bioavailability by enhancing BH_4 levels via DHFR. These findings are in agreement with previous in vivo (11) and in vitro studies (11,38) showing that DHFR plays a key role in regulating the BH_4-to-BH_2 ratio and eNOS coupling under conditions of low total BH_4 availability. For example, in endothelial cells (38,40) expressing eNOS with low BH_4 levels, DHFR inhibition or knockdown further diminished the BH_4-to-BH_2 ratio and exacerbated eNOS uncoupling.

Reduced BH_4 availability in ihMCs could also be attributed to reduced BH_4 stability. Diminished BH_4 stability has been reported in endothelial dysfunction (41) as well as in rats with DN (6). HG levels, as seen in diabetic conditions,

increase the formation of superoxide through one main source in the kidney, NADPH oxidase activation. NO produced by eNOS and superoxide combine to form peroxynitrite anions. Oxidation of BH_4 by ROS, such as peroxynitrite, results in BH_2 formation, which inactivates the eNOS cofactor function, suggesting that reduced BH_4 stability uncouples eNOS and leads to reduced NO bioavailability and a further rise in the formation of diabetic glomeruli superoxides.

In conclusion, the current work indicates that GT reverses diabetes-induced uncoupling eNOS as experienced in renal mesangial cells exposed to HG levels and SHR diabetic rats. GT seems to ameliorate uncoupling eNOS via a rise in BH_4 levels/reduction in BH_4 oxidation, which occurs as a result of the de novo synthesis of BH_4. A rise in BH_4 levels would account, then, for reduced eNOS uncoupling leading to the amelioration of oxidative stress and enhanced NO availability.

ACKNOWLEDGMENTS

This work was supported by the Fundação de Amparo à Pesquisa do Estado de São Paulo (Grant 2008/57560-0) and Conselho Nacional de Desenvolvimento Científico e Tecnológico (CNPq). A.M.F. received a scholarship from CNPq.

No potential conflicts of interest relevant to this article were reported.

A.M.F., A.P., and K.C.S. acquired the data and wrote the manuscript. J.M.L.F. contributed to discussion and reviewed the manuscript. J.B.L.F. designed the study, reviewed the data, and wrote, reviewed, and edited the manuscript. J.B.L.F. is the guarantor of this work and, as such, had full access to all of the data in the study and takes responsibility for the integrity of the data and the accuracy of the data analysis.

The authors thank Luciana Cristina Teixeira (Department of Medicine, Nephrology Division, Federal University of São Paulo, Brazil) for helping with the culture of the ihMC line and are grateful to Dr. Ricardo Pereira and Dr. Marcelo Ganzarolli de Oliveira (Laboratory of Liquid Chromatography, Institute of Chemistry, University of Campinas [Unicamp], Campinas, SP, Brazil) for their technical and scientific assistance. The authors are very grateful to the personnel from the Renal Pathophysiology Laboratory, Investigation on Diabetes Complications, Faculty of Medical Sciences (FCM), Unicamp, for their invaluable help with this work. In particular, the authors are very grateful to Dr. Elisa E.M. Peixoto (Renal Pathophysiology Laboratory, Unicamp), for blindly estimating the extracellular matrix expansion in kidney slides.

REFERENCES

1. Brownlee M. The pathobiology of diabetic complications: a unifying mechanism. Diabetes 2005;54:1615–1625
2. Lopes de Faria JB, Silva KC, Lopes de Faria JM. The contribution of hypertension to diabetic nephropathy and retinopathy: the role of inflammation and oxidative stress. Hypertens Res 2011;34:413–422
3. Nishikawa T, Edelstein D, Du XL, et al. Normalizing mitochondrial superoxide production blocks three pathways of hyperglycaemic damage. Nature 2000;404:787–790
4. Guzik TJ, Mussa S, Gastaldi D, et al. Mechanisms of increased vascular superoxide production in human diabetes mellitus: role of NAD(P)H oxidase and endothelial nitric oxide synthase. Circulation 2002;105:1656–1662
5. Ribaldo PDB, Souza DS, Biswas SK, Block K, Lopes de Faria JM, Lopes de Faria JB. Green tea (*Camellia sinensis*) attenuates nephropathy by downregulating Nox4 NADPH oxidase in diabetic spontaneously hypertensive rats. J Nutr 2009;139:96–100
6. Satoh M, Fujimoto S, Haruna Y, et al. NAD(P)H oxidase and uncoupled nitric oxide synthase are major sources of glomerular superoxide in rats with experimental diabetic nephropathy. Am J Physiol Renal Physiol 2005; 288:F1144–F1152
7. Komers R, Anderson S. Glomerular endothelial NOS (eNOS) expression in type 2 diabetic patients with nephropathy. Nephrol Dial Transplant 2008; 23:3037
8. Komers R, Anderson S. Paradoxes of nitric oxide in the diabetic kidney. Am J Physiol Renal Physiol 2003;284:F1121–F1137
9. Zweier JL, Chen CA, Druhan LJ. S-glutathionylation reshapes our understanding of endothelial nitric oxide synthase uncoupling and nitric oxide/reactive oxygen species-mediated signaling. Antioxid Redox Signal 2011;14:1769–1775
10. Crabtree MJ, Hale AB, Channon KM. Dihydrofolate reductase protects endothelial nitric oxide synthase from uncoupling in tetrahydrobiopterin deficiency. Free Radic Biol Med 2011;50:1639–1646
11. Thöny B, Auerbach G, Blau N. Tetrahydrobiopterin biosynthesis, regeneration and functions. Biochem J 2000;347:1–16
12. Schmidt TS, Alp NJ. Mechanisms for the role of tetrahydrobiopterin in endothelial function and vascular disease. Clin Sci (Lond) 2007;113:47–63
13. Crabtree MJ, Smith CL, Lam G, Goligorsky MS, Gross SS. Ratio of 5,6,7,8-tetrahydrobiopterin to 7,8-dihydrobiopterin in endothelial cells determines glucose-elicited changes in NO vs. superoxide production by eNOS. Am J Physiol Heart Circ Physiol 2008;294:H1530–H1540
14. Xu J, Wu Y, Song P, Zhang M, Wang S, Zou MH. Proteasome-dependent degradation of guanosine 5′-triphosphate cyclohydrolase I causes tetrahydrobiopterin deficiency in diabetes mellitus. Circulation 2007;116:944–953
15. Werner ER, Blau N, Thöny B. Tetrahydrobiopterin: biochemistry and pathophysiology. Biochem J 2011;438:397–414
16. Nakagawa T, Tanabe K, Croker BP, et al. Endothelial dysfunction as a potential contributor in diabetic nephropathy. Nat Rev Nephrol 2011;7:36–44
17. Schmitt CA, Dirsch VM. Modulation of endothelial nitric oxide by plant-derived products. Nitric Oxide 2009;21:77–91
18. Widlansky ME, Hamburg NM, Anter E, et al. Acute EGCG supplementation reverses endothelial dysfunction in patients with coronary artery disease. J Am Coll Nutr 2007;26:95–102
19. Cooper ME, Allen TJ, Macmillan P, Bach L, Jerums G, Doyle AE. Genetic hypertension accelerates nephropathy in the streptozotocin diabetic rat. Am J Hypertens 1988;1:5–10
20. Peixoto EB, Pessoa BS, Biswas SK, Lopes de Faria JB. Antioxidant SOD mimetic prevents NADPH oxidase-induced oxidative stress and renal damage in the early stage of experimental diabetes and hypertension. Am J Nephrol 2009;29:309–318
21. Cristovam PC, Arnoni CP, de Andrade MC, et al. ACE-dependent and chymase-dependent angiotensin II generation in normal and glucose-stimulated human mesangial cells. Exp Biol Med (Maywood) 2008;233: 1035–1043
22. Bradford MM. A rapid and sensitive method for the quantitation of microgram quantities of protein utilizing the principle of protein-dye binding. Anal Biochem 1976;72:248–254
23. Komers R, Schutzer WE, Reed JF, et al. Altered endothelial nitric oxide synthase targeting and conformation and caveolin-1 expression in the diabetic kidney. Diabetes 2006;55:1651–1659
24. Miranda KM, Espey MG, Wink DA. A rapid, simple spectrophotometric method for simultaneous detection of nitrate and nitrite. Nitric Oxide 2001; 5:62–71
25. Fukushima T, Nixon JC. Analysis of reduced forms of biopterin in biological tissues and fluids. Anal Biochem 1980;102:176–188
26. Fekkes D, Voskuilen-Kooijman A. Quantitation of total biopterin and tetrahydrobiopterin in plasma. Clin Biochem 2007;40:411–413
27. Vann LR, Twitty S, Spiegel S, Milstien S. Divergence in regulation of nitric-oxide synthase and its cofactor tetrahydrobiopterin by tumor necrosis factor-α. Ceramide potentiates nitric oxide synthesis without affecting GTP cyclohydrolase I activity. J Biol Chem 2000;275:13275–13281
28. Goto T, Yoshida Y, Kiso M, Nagashima H. Simultaneous analysis of individual catechins and caffeine in green tea. J Chomatogr 1996;749:295–299
29. Förstermann U. Nitric oxide and oxidative stress in vascular disease. Pflugers Arch 2010;459:923–939
30. Mattar AL, Fujihara CK, Ribeiro MO, de Nucci G, Zatz R. Renal effects of acute and chronic nitric oxide inhibition in experimental diabetes. Nephron 1996;74:136–143
31. Tolins JP, Shultz PJ, Raij L, Brown DM, Mauer SM. Abnormal renal hemodynamic response to reduced renal perfusion pressure in diabetic rats: role of NO. Am J Physiol 1993;265:F886–F895
32. Nakagawa T, Sato W, Glushakova O, et al. Diabetic endothelial nitric oxide synthase knockout mice develop advanced diabetic nephropathy. J Am Soc Nephrol 2007;18:539–550

33. Ott C, Schneider MP, Delles C, Schlaich MP, Schmieder RE. Reduction in basal nitric oxide activity causes albuminuria. Diabetes 2011;60:572–576
34. Thomas SR, Witting PK, Drummond GR. Redox control of endothelial function and dysfunction: molecular mechanisms and therapeutic opportunities. Antioxid Redox Signal 2008;10:1713–1765
35. Oubaha M, Gratton JP. Phosphorylation of endothelial nitric oxide synthase by atypical PKC zeta contributes to angiopoietin-1-dependent inhibition of VEGF-induced endothelial permeability in vitro. Blood 2009; 114:3343–3351
36. Schulz E, Jansen T, Wenzel P, Daiber A, Münzel T. Nitric oxide, tetrahydrobiopterin, oxidative stress, and endothelial dysfunction in hypertension. Antioxid Redox Signal 2008;10:1115–1126
37. Noguchi K, Hamadate N, Matsuzaki T, et al. Improvement of impaired endothelial function by tetrahydrobiopterin in stroke-prone spontaneously hypertensive rats. Eur J Pharmacol 2010;631:28–35
38. Crabtree MJ, Tatham AL, Hale AB, Alp NJ, Channon KM. Critical role for tetrahydrobiopterin recycling by dihydrofolate reductase in regulation of endothelial nitric-oxide synthase coupling: relative importance of the de novo biopterin synthesis versus salvage pathways. J Biol Chem 2009;284: 28128–28136
39. Okumura M, Masada M, Yoshida Y, et al. Decrease in tetrahydrobiopterin as a possible cause of nephropathy in type II diabetic rats. Kidney Int 2006; 70:471–476
40. Sugiyama T, Levy BD, Michel T. Tetrahydrobiopterin recycling, a key determinant of endothelial nitric-oxide synthase-dependent signaling pathways in cultured vascular endothelial cells. J Biol Chem 2009;284: 12691–12700
41. Landmesser U, Dikalov S, Price SR, et al. Oxidation of tetrahydrobiopterin leads to uncoupling of endothelial cell nitric oxide synthase in hypertension. J Clin Invest 2003;111:1201–1209